ARTICLE IN PRESS

Inorganica Chimica Acta xxx (2016) xxx–xxx

Contents lists available at ScienceDirect

Inorganica Chimica Acta

journal homepage: www.elsevier.com/locate/ica

Synthesis, structures and catalytic activity of *p*-tolylimido rhenium(V) complexes incorporating quinoline-derived ligands

I. Gryca [a], B. Machura [a,*], Lidia S. Shul'pina [b], Georgiy B. Shul'pin [c,d,*]

[a] Department of Crystallography, Institute of Chemistry, University of Silesia, 9th Szkolna St., 40-006 Katowice, Poland
[b] Nesmeyanov Institute of Organoelement Compounds, Russian Academy of Sciences, ulitsa Vavilova, dom 28, Moscow 119991, Russia
[c] Semenov Institute of Chemical Physics, Russian Academy of Sciences, ulitsa Kosygina, dom 4, Moscow 119991, Russia
[d] Plekhanov Russian University of Economics, Stremyannyi pereulok, dom 36, Moscow 117997, Russia

ARTICLE INFO

Article history:
Received 19 February 2016
Received in revised form 13 April 2016
Accepted 18 April 2016
Available online xxxx

This paper is dedicated to the memory of Professor Rino Michelin.

Keywords:
Rhenium imido complexes
X-ray structure
DFT calculations
Alcohols
tert-Butyl hydroperoxide
Oxidation

ABSTRACT

p-Tolylimido rhenium(V) complexes, *trans*-(Cl,Cl)-[Re(*p*-$NC_6H_4CH_3$)Cl_2(4-MeO-quin-2-COO)(PPh_3)] (**1**), *trans*-(Br,Br)-[Re(*p*-$NC_6H_4CH_3$)Br_2(4-MeO-quin-2-COO)(PPh_3)]·2MeCN (**2**), *trans*-(Cl,Cl)-[Re(*p*-$NC_6H_4CH_3$)Cl_2(isoquin-1-COO)(PPh_3)] (**3**), *trans*-(Br,Br)-[Re(*p*-$NC_6H_4CH_3$)Br_2(isoquin-1-COO)(PPh_3)] (**4**), *cis*-(Cl,Cl)-[Re(*p*-$NC_6H_4CH_3$)Cl_2(4-MeO-quin-2-COO)(PPh_3)] (**5**), *cis*-(Br,Br)-[Re(*p*-$NC_6H_4CH_3$)Br_2(4-MeO-quin-2-COO)(PPh_3)]·MeOH (**6**), *cis*-(Cl,Cl)-[Re(*p*-$NC_6H_4CH_3$)Cl_2(isoquin-1-COO)(PPh_3)] (**7**) and *cis*-(Br,Br)-[Re(*p*-$NC_6H_4CH_3$)Br_2(isoquin-1-COO)(PPh_3)] (**8**), have been synthesized and characterized using X-ray analysis and spectroscopic methods (IR, ^1H, ^{13}C and ^{31}P NMR, UV–Vis). To elucidate the structural, spectroscopic and bonding properties, the theoretical calculations at the DFT level were undertaken for **1**, **3**, **5** and **7**. The synthesized complexes exhibited moderate activity in the oxidation of 1-phenylethanol and certain alkanes (*n*-heptane and methylcyclohexane) with *tert*-butyl hydroperoxide (TBHP) in acetonitrile. Chromatograms of products obtained from the alkanes indicated that a sufficient sterical hindrance exists around of the rhenium catalytic center.

1. Introduction

Transition metal complexes containing multiple bonds to oxygen and nitrogen atoms attract widespread scientific attention. These compounds have been postulated as the active intermediates in biologically relevant transformations [1] and they were successfully employed as effective catalysts in numerous industrial processes [2]. The high-oxidation state of the catalyst allows the reaction to be carried out under "open-flask" conditions, without the need for rigorous exclusion of air and moisture.

Particular attention has been drawn to high-oxidation state rhenium complexes. The rhenium(VII) derivative methylrhenium trioxide in combination with hydrogen peroxide has found wide use in oxidation catalysis. Rhenium complexes have become important catalysts for oxidation of various organic compounds [3] including olefins, ketones and alcohols. High-valent oxo-rhenium complexes were also successfully employed in the activation of C—H bonds of aromatic and saturated hydrocarbons [4]. In recent years, there has been also a renewed interest in high-valent imido rhenium complexes [5]. Imido (NR^{2-}) ligands are isoelectronic to oxo (O^{2-}) ions. Compared to oxo complexes, however, imido complexes seems to be more versatile due to an opportunity to tune the steric and electronic properties of the complex by changing the nitrogen substituent [6].

Recently [7], we reported the synthesis and properties of several imidorhenium(V) complexes incorporating uninegative bidentate N,O-chelating ligands. The studies demonstrated that compounds [Re(*p*-$NC_6H_4CH_3$)X_3(PPh_3)$_2$] (X = Cl, Br) are excellent starting materials for the syntheses of these compounds and that the reaction course of [Re(*p*-$NC_6H_4CH_3$)X_3(PPh_3)$_2$] with N,O-donor chelating ligands is governed by many factors, including the type of the ligand and experimental conditions. The complexes [Re(*p*-$NC_6H_4CH_3$)X_2(pyz-2-COO)(PPh_3)] and [Re(*p*-$NC_6H_4CH_3$)X_2(ind-3-COO)(PPh_3)] were found to catalyze oxidation of alkanes with H_2O_2 and *tert*-butyl hydroperoxide (TBHP) and of alcohols with TBHP, whereas [Re(*p*-$NC_6H_4CH_3$)X_2(py-2-COO)(PPh_3)] exhibited catalytic activity in the syntheses of *N*-substituted ethyl glycine esters from ethyl diazoacetate and amines. Noteworthy, the catalytic activity of these systems may be influenced by different

---

* Corresponding authors at: Semenov Institute of Chemical Physics, Russian Academy of Sciences, ulitsa Kosygina, dom 4, Moscow 119991, Russia (G.B. Shul'pin).

E-mail addresses: basia@ich.us.edu.pl (B. Machura), Shulpin@chph.ras.ru (G.B. Shul'pin).

http://dx.doi.org/10.1016/j.ica.2016.04.030
0020-1693/© 2016 Published by Elsevier B.V.

Please cite this article in press as: I. Gryca et al., Inorg. Chim. Acta (2016), http://dx.doi.org/10.1016/j.ica.2016.04.030

regio-isomers (*cis*-(X,X) or *trans*-(X,X)) of [Re(p-$NC_6H_4CH_3$)X_2(N—O)(PPh_3)]. In the present studies, we used another bidentate chelating carboxylate ligands incorporating quinoline or isoquinoline ring, namely isoquinoline-1-carboxylic acid (iqcH) and 4-methoxy-2-quinolinecarboxylic acid (mqcH).

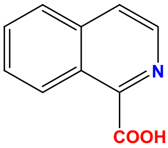

Isoquinoline-1-carboxylic acid
(iqcH)

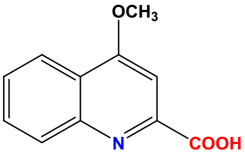

4-Methoxy-2-quinolinecarboxylic
acid (mqcH)

Herein, we present the structural, spectroscopic and catalytic properties of the following imido complexes: *trans*-(Cl,Cl)-[Re(p-$NC_6H_4CH_3$)Cl_2(4-MeO-quin-2-COO)(PPh_3)] (**1**), *trans*-(Br,Br)-[Re(p-$NC_6H_4CH_3$)Br_2(4-MeO-quin-2-COO)(PPh_3)]·2MeCN (**2**), *trans*-(Cl,Cl)-[Re(p-$NC_6H_4CH_3$)Cl_2(isoquin-1-COO)(PPh_3)] (**3**), *trans*-(Br,Br)-[Re(p-$NC_6H_4CH_3$)Br_2(isoquin-1-COO)(PPh_3)] (**4**), *cis*-(Cl,Cl)-[Re(p-$NC_6H_4CH_3$)Cl_2(4-MeO-quin-2-COO)(PPh_3)] (**5**), *cis*-(Br,Br)-[Re(p-$NC_6H_4CH_3$)Br_2(4-MeO-quin-2-COO)(PPh_3)]·MeOH (**6**), *cis*-(Cl,Cl)-[Re(p-$NC_6H_4CH_3$)Cl_2(isoquin-1-COO)(PPh_3)] (**7**) and *cis*-(Br,Br)-[Re(p-$NC_6H_4CH_3$)Br_2(isoquin-1-COO)(PPh_3)] (**8**). To get a better understanding of the structural, spectroscopic and bonding properties, the theoretical calculations at the DFT level were undertaken for **1**, **3**, **5** and **7**. The catalytic potential of the complexes in oxidations was studied.

2. Results and discussion

2.1. Synthesis of the complexes

The complexes **1**–**8** were prepared in good yield by ligand exchange reactions of *mer*-[Re(p-$NC_6H_4CH_3$)X_3(PPh_3)$_2$] or *trans*-(X,X)-[Re(p-$NC_6H_4CH_3$)X_2(OMe)(PPh_3)$_2$] with 4-methoxy-2-quinolinecarboxylic acid (4-MeO-quin-2-COOH) and isoquinoline-1-carboxylic acid (isoquin-1-COOH), respectively (Scheme 1). The synthetic strategy of **1**–**8** is presented in Scheme 1.

As in the previous studies [7c,f,g], the reactions of *mer*-[Re(p-$NC_6H_4CH_3$)X_3(PPh_3)$_2$] with N-heterocyclic acids (4-MeO-quin-2-COOH and isoquin-1-COOH) were independent on molar ratio of the metal precursor to ligand. Even when excess of the acid was used, only monosubstituted compounds of general formula [Re(p-$NC_6H_4CH_3$)X_2(N—O)(PPh_3)] were obtained. Formation of isomeric forms (*trans*–*cis*) of [Re(p-$NC_6H_4CH_3$)X_2(4-MeO-quin-2-COO)(PPh_3)] and [Re(p-$NC_6H_4CH_3$)Cl_2(isoquin-1-COO)(PPh_3)] were found to be solvent-dependent. Refluxing of *mer*-[Re(p-$NC_6H_4CH_3$)X_3(PPh_3)$_2$] with 4-MeO-quin-2-COOH and isoquin-1-COOH in acetonitrile led to the compounds [Re(p-$NC_6H_4CH_3$)X_2(N—O)(PPh_3)] (N—O = 4-MeO-quin-2-COO or isoquin-1-COO) with halide ions in *trans* arrangement, whereas the mixture of *cis* and *trans* isomers of [Re(p-$NC_6H_4CH_3$)X_2(4-MeO-quin-2-COO)(PPh_3)] and [Re(p-$NC_6H_4CH_3$)Cl_2(isoquin-1-COO)(PPh_3)] were isolated from the reactions carried out in methanolic solution. These findings are consistent with those reported for [Re(p-$NC_6H_4CH_3$)X_2(py-2-COO)(PPh_3)] [7f]. Different reactivity pattern in acetonitrile and methanol is attributed to formation of *trans*-(X,X)-[Re(p-$NC_6H_4CH_3$)X_2(OMe)(PPh_3)$_2$] in the reaction of *mer*-[Re(p-$NC_6H_4CH_3$)X_3(PPh_3)$_2$] with methanol and subsequent reaction of *trans*-(X,X)-[Re(p-$NC_6H_4CH_3$)X_2(OMe)(PPh_3)$_2$] with N-heterocyclic acid. In acetonitrile, the first step seems to concern the substitution of the labile X ligand *trans* to the imido group in *mer*-[Re(p-$NC_6H_4CH_3$)X_3(PPh_3)$_2$] by the oxygen atom of N,O-donor ligand, possibly with the proton transfer to the released X^-. In the next step, the uncoordinated N-donor atom of N,O-donor ligand substitutes the equatorial phosphine to form neutral imido complex *trans*-(X,X)-[Re(p-$NC_6H_4CH_3$)X_2(N-O)(PPh_3)$_2$]. In methanol, the labile X ligand *trans* to the imido group in *mer*-[Re(p-$NC_6H_4CH_3$)X_3(PPh_3)$_2$] can be substituted by both oxygen atom of N,O-donor ligand and the methoxy ion coming from methanol. As for [Re(p-$NC_6H_4CH_3$)X_2(py-2-COO)(PPh_3)], the reactions of *trans*-(X,X)-[Re(p-$NC_6H_4CH_3$)X_2(OMe)(PPh_3)$_2$] with N-heterocyclic acids (4-MeO-quin-2-COOH and isoquin-1-COOH) resulted in the formation of *cis* isomers (Scheme 2).

All complexes **1**–**8** show high stability toward air and moisture both in the solid state and in solution for several weeks at ambient temperature. They are moderately soluble in polar solvents such as acetonitrile, acetone, chloroform, dichloromethane and methanol, as well as non-polar solvents as benzene.

2.2. IR and ^{1}H NMR spectra

The IR spectra of **1**–**8** are dominated by very strong band that occurs in range 1684–1698 cm^{-1} assigned to $\nu_{as}(CO_2)$ stretching mode and two strong $\nu_s(CO_2)$ bands found in the range 1241–1330 cm^{-1}. High values of $\Delta\nu(CO_2) = \nu_{as}(CO_2) - \nu_s(CO_2)$ (350–430 cm^{-1}) reflect a unidentate coordination mode of the carboxylate group in compounds **1**–**8** [8]. For both *trans*-(X,X) and *cis*-(X,X) isomers of [Re(p-$NC_6H_4CH_3$)X_2(4-MeO-quin-2-COO)(PPh_3)] and [Re(p-$NC_6H_4CH_3$)X_2(isoquin-1-COO)(PPh_3)], these frequencies are very similar and they are not distinctive for molecular structure determination. The vibrations ν(Re—$NC_6H_4CH_3$) in **1**–**8** are difficult to identify experimentally as they are mixed with $\nu_{C=N}$ and $\nu_{P—C}$ modes of PPh_3 and 4-MeO-quin-2-COO^- and isoquin-1-COO^- ligands [7b–d,9].

In the ^{1}H NMR spectra of the examined compounds distinctive signals corresponding to the alkyl protons of the p-tolylimido group occur in the range 2.30–2.21 ppm. The signals of alkyl protons of the 4-methoxy-2-quinolinecarboxylate ligand of **1**, **2**, **5** and **6** complexes occur in the range 4.32–4.14 ppm. The protons of PPh_3 appear in the range 7.71–7.11 ppm. The signals of 4-methoxyquinoline and isoquinoline hydrogens, that appear in the range 8.29–6.95 and 9.50–7.73 ppm, respectively, are shifted downfield in comparison with the free ligands (8.08–6.49 ppm for 4-methoxyquinoline ligand and 8.96–7.65 ppm for isoquinoline ligand).

The coordination of the phosphine was additionally confirmed by ^{31}P NMR spectroscopy. As expected, the single phosphorus signals, observed for **1**–**8** in the range 25.42–25.81 ppm, are downfield from uncoordinated triphenylphosphine (−6 ppm). The lack of paramagnetic broadening or shifts of resonances in the ^{1}H NMR spectra of **1**–**8** is in agreement with diamagnetism of the complexes.

2.3. Molecular structures

A definite proof for the structures of **1**–**8** is provided by the X-ray diffraction data. The crystallographic parameters of **1**–**8** are summarized in Table 1. The perspective drawings of the asymmetric

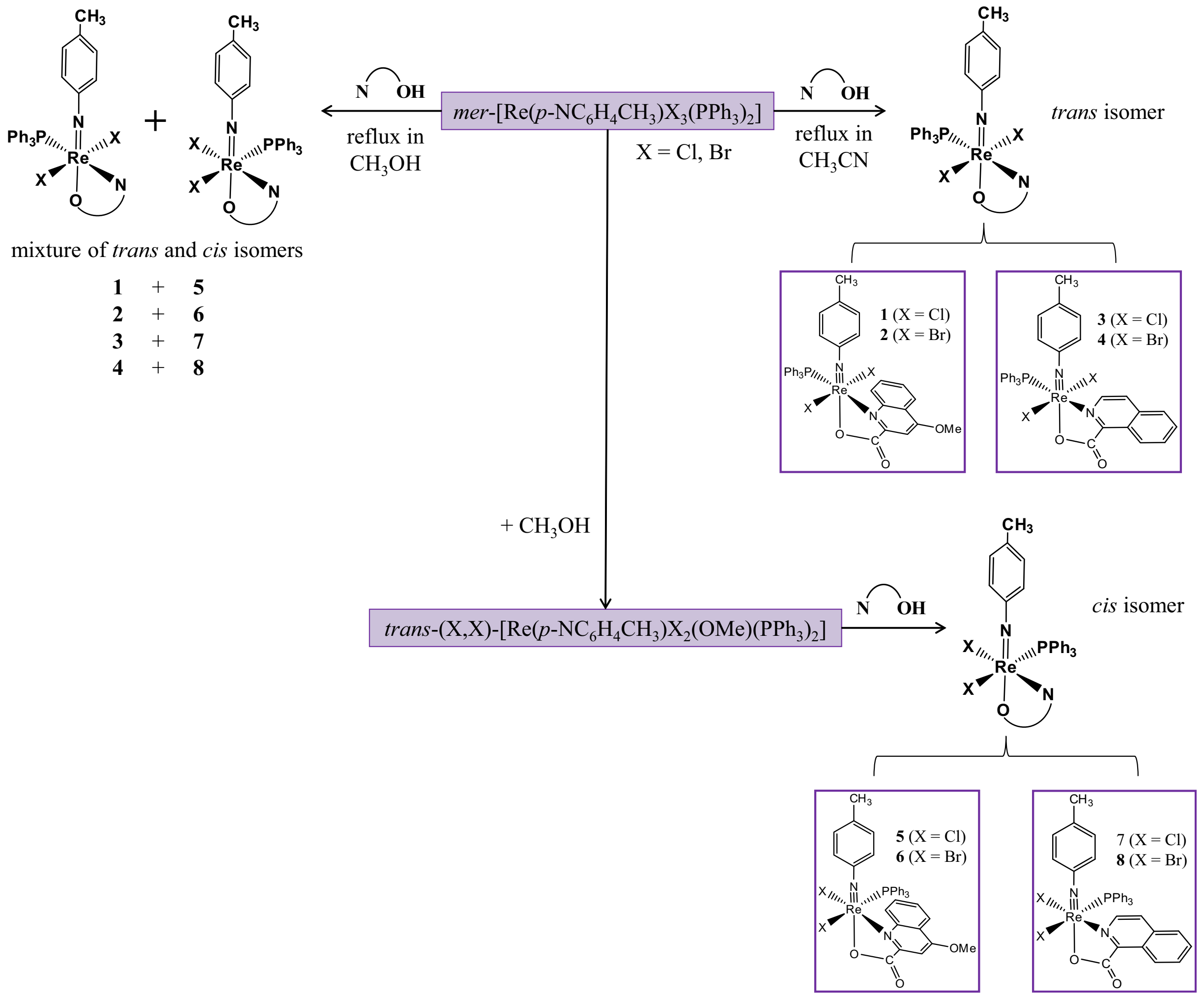

Scheme 1. Formation of complexes **1–8**.

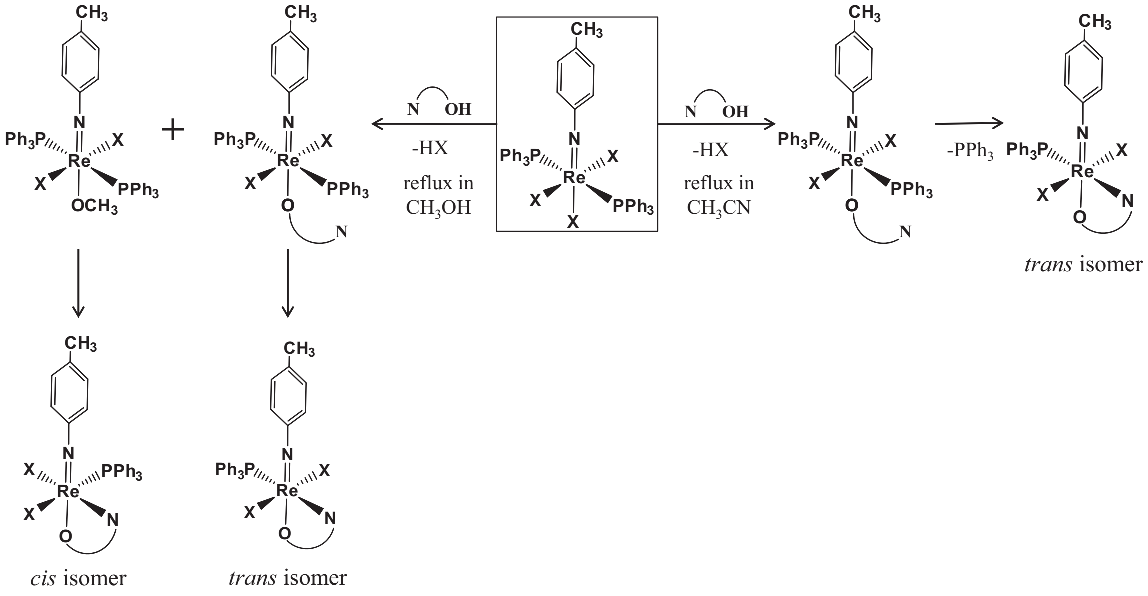

Scheme 2. Proposed mechanism for the formation of *cis* or *trans*-(X,X)-[Re(p-NC$_6$H$_4$CH$_3$)X$_2$(N–O)(PPh$_3$)] (N–O = 4-MeO-quin-2-COO$^-$ or isoquin-1-COO$^-$).

Please cite this article in press as: I. Gryca et al., Inorg. Chim. Acta (2016), http://dx.doi.org/10.1016/j.ica.2016.04.030

units of **1**–**8** are presented in Fig. 1, and the selected bond distances and angles are collected in Table 2.

All reported complexes show a six-coordinate rhenium atom with distorted octahedral geometries defined by the *p*-methylphenylimido group, two halide ions, the phosphorus atom of PPh_3 molecule, and the carboxylate chelate ligand 4-MeO-quin-2-COO$^-$ (in **1**, **2**, **5** and **6**) or isoquin-1-COO$^-$ (in **3**, **4**, **7** and **8**). The principal distortions result from the presence of multiple *p*-methylphenylimido ligand and bite angles of bidentate ligands 4-MeO-quin-2-COO$^-$ or isoquin-1-COO$^-$ coordinating through the nitrogen and oxygen atoms (with the bite angle of 74.81(10) in **1**, 75.6(2) in **2**, 74.62(17) in **3**, 75.2(3) in **4**, 74.53(12) in **5**, 74.64(13) in **6**, 74.32(19) in **7** and 74.75(14)° in **8**). For all examined complexes **1**–**8**, the Re—N$_{\text{imido}}$ bond lengths (from 1.700(4) Å in **8** to 1.726(7) Å in **2**) fall in the range 1.67–1.74 Å typical for mononuclear complexes of rhenium(V) having $[\text{Re}{\equiv}\text{NR}]^{3+}$ core, and reflect the expected triple Re≡N bond. The triply bonded *p*-methylphenylimido ligand forces the metal nonbonding d electrons to lie in the plane perpendicular to the Re≡NR bond axis. Due to accessible π-donation from the rhenium ion, triphenylphosphine molecule and π-acceptor N-heterocyclic ring of the bidentate ligand adopt *cis* disposition with respect to the linear Re≡NR core. The presence of the harder oxygen atom of the chelating N,O-donor ligand in the *trans* position to the ion *p*-$NC_6H_4CH_3$ is justified by *trans*-influence of the imido group. The complexes **1**–**4** were found to be the *trans* isomer of [Re(*p*-$NC_6H_4CH_3$)X_2(N—O)(PPh_3)], whereas the halide ligands of **5**–**8** occupy *cis* positions to each other. As previously reported [7g], the energy difference between *trans*-(X,X) and *cis*-(X,X) isomers of [Re(*p*-$NC_6H_4CH_3$)X_2(N—O)(PPh_3)] is remarkably small indicating that their formation is kinetically rather than thermodynamically controlled. Also, a search in the CSD (The Cambridge Structural Database, Version 5.36) confirms that both isomeric forms are almost equally observed among [Re(NR)X_2(N—O)(PPh_3)] complexes. The most important structural parameters of [Re(*p*-NR)X_2(N—O)(PPh_3)] are gathered in Table S1.

The Re—N, Re—X, Re—O and Re—O bond lengths of **1**–**8** are within the expected range for [Re(NR)X_2(N—O)(PPh_3)] complexes (Tables 2 and S1; see also Refs. [7,9a,10]). In all reported complexes the Re—N bonds are significantly longer than the Re—O distances. This effect occurs in complexes of metal ions in high oxidation state and can be understood in terms of Pearson's hard-soft acid–base theory. As hard Lewis acid Re^{V} ion forms stronger bonds with oxygen rather than with the comparatively softer base nitrogen donor. Importantly, the interatomic distance between the rhenium atom and the carboxylate oxygen atom in **1**–**8** is almost equal to an ideal single Re—O bond length (ca. 2.04 Å) [11], indicating lack of delocalization in the RN≡Re—O unit. The Re—N$_{\text{imido}}$—C$_{\text{imido}}$ bond angles of 173.38(11)° in **1**, 176.1(3)° in **2**, 178.2(2)° in **3**, 178.0(3)° in **4**, 170.39(17)° in **5**, 169.73(18)° in **6**, 167.3(2)° in **7** and 168.40(16)° in **8** agree with a linear coordination mode of the arylimido ligands, and these values are typical of phenyl imido ligands in high oxidation state complexes, in which the metal is relatively electron-deficient and some π-bonding between the imido nitrogen atom and the metal is likely. Finally, no extraordinary differences in terms of bond lengths and angles can be noticed between *trans*-(X,X)-[Re(*p*-$NC_6H_4CH_3$)X_2(N-COO)(PPh_3)] and *cis*-(X,X)-[Re(*p*-$NC_6H_4CH_3$)Cl_2(N-COO)(PPh_3)] compounds. No intermolecular interactions with enough strength to govern crystal packing or molecule conformation were found in the structures of **1**–**8** except for weak intra- and intermolecular C—H···Cl, C—H···N type and C—H···O contacts (Table S2).

2.4. DFT calculations

For further understanding structural and bonding properties of the imido rhenium(V) complexes, the calculations at the DFT level were undertaken for **1**, **3**, **5** and **7**.

As presented in Tables S3 and S4, the PBE1PBE method gives acceptable deviations between the experimental and theoretical geometric data. The Re—N$_{\text{imido}}$ bond lengths are reproduced with small deviations ranging from +0.001 to +0.005 Å. Also, the experimental and calculated spectra of **1**, **3**, **5** and **7** are in reasonable agreement (Fig. S1). The calculated $\nu_{as}(CO_2)$ and $\nu_s(CO_2)$ are almost identical for both *trans*-(X,X) and *cis*-(X,X), despite the different molecular symmetry of these isomers (1814, 1333 and 1306 cm^{-1} for **1** and 1806, 1331 and 1306 cm^{-1} for **5**; 1808, 1312 and 1287 cm^{-1} for **3** and 1800, 1312 and 1287 cm^{-1} for **7**). In comparison with the experimental data, these values are shifted to higher frequencies by ~7%, which is an usual feature for this approach (Fig. S1). The calculated ν(Re—$NC_6H_4CH_3$) frequencies appear at 1553, 1439 and 1062 cm^{-1} for **1**, 1555, 1453 and 1065 cm^{-1} for **3**, 1556, 1453 and 1065 cm^{-1} for **5** and 1554, 1453 and 1065 cm^{-1} for **7**. As mentioned above, experimentally these vibrations are difficult to identify as the ν(Re—$NC_6H_4CH_3$) stretches are mixed with $\nu_{C=N}$ and $\nu_{P—C}$ modes of PPh_3 and isoquin-1-COO$^-$ and 4-MeO-quin-2-COO$^-$ ligands [5d,e,12].

To get additional insight into the bond characteristics in the reported compounds, a natural bond orbital (NBO) study was performed. The occupancy and composition of the calculated Re—N(2) natural bond orbitals (NBOs) are given in Table S5. For complexes **1**, **5** and **7**, the results of NBO point to the existence of one σ and two π natural Re—N$_{\text{imido}}$ orbitals, whereas for complex **3** NBO results reveal only two Re—NR natural bond orbitals. Both orbitals of **3** result from overlapping of the empty d_{xy} and d_{yz} rhenium orbitals with the occupied p_x and p_z orbitals of the deprotonated nitrogen of the imido ligand, and they are of π character. Lack of σ Re—NR natural orbital indicates a conceivable predominant Coulomb-type Re—ligand interaction. σ and π bonds of **1**, **5** and **7** as well as π bonds of **3** are strongly polarized toward the nitrogen atom; the nitrogen contributions to these bonds are between 57% and 73%. The hybridization at rhenium shows clearly that d contribution dominates the metal bonding in σ and π Re—N$_{\text{imido}}$ bonds. For π bonds, the oxygen atom employs pure or quasi pure π atomic orbitals. The nature of Re—N$_{\text{imido}}$ bonds is in agreement with the results obtained in previous works regarding analysis of the bonding nature of imido rhenium(V) complexes.

For all complexes, the Wiberg bond indices of the Re—N(2) are almost three times larger than those of Re(1)—N(1) and Re(1)—O(1). The values 2.069 for **1**, 2.085 for **3**, 2.051 for **5**, and 2.056 for **7** are consistent with a formal Re═N double-bond description, with a partial triple-bond character. The WBIs of the Re(1)—O(1) and Re(1)—N(1) bonds are in the range of 0.5–0.6. A greater degree of covalent character is evidenced by WBIs for bonds between the central ion and halide or triphenylphosphine ligand (Table S6).

Schematic representation of the energy of the highest occupied and lowest unoccupied orbitals of **1**, **3**, **5** and **7** is presented in Fig. S2. The contours of the selected frontier orbitals of **1**, **3**, **5** and **7** are depicted in Fig. 2, whereas their percentage compositions are gathered in Table S7. The HOMO of all examined complexes presents significant metallic character (60%), and its energy is almost unaffected by the nature of the carboxylate ligand and symmetry of the compound. Except for **3**, the HOMO is constituted by rhenium d_{xy} orbital in antibonding relation to the occupied p orbital of Cl ligand and occupied p orbital of carboxylate oxygen atom. What is more, the HOMO orbitals of **1**, **5** and **7** present a similar percentage contribution, 60% d(Re), 30% π(Cl) and 10% π(N—O) for **1**, 60% d(Re), 25% π(Cl) and 15% π(N—O) for **5** and 50% d(Re), 35% π(Cl) and 15% π(N—O) for **7**. In contrast, the HOMO of **3** is a nonbonding combination of rhenium d_{xy} orbital p chloride orbitals. To a large extent, the H-1 of **1**, **5** and **7** can be considered as $\pi_{\text{Re}\equiv\text{NR}}$ orbitals. It consists of d_π of rhenium and π orbitals of the imido ligand. For both isomers, H-1 molecular orbital is contributed by p chloride orbitals. The H-1 orbital of **3** is mainly contributed by

Please cite this article in press as: I. Gryca et al., Inorg. Chim. Acta (2016), http://dx.doi.org/10.1016/j.ica.2016.04.030

Table 1
Crystal data and structure refinement for **1**–**8** complexes.

	1	**2**	**3**	**4**	**5**	**6**	**7**	**8**
Empirical formula	$C_{36}H_{30}Cl_2N_2O_3PRe$	$C_{40}H_{36}Br_2N_4O_3PRe$	$C_{35}H_{28}Cl_2N_2O_2PRe$	$C_{35}H_{28}Br_2N_2O_2PRe$	$C_{36}H_{30}Cl_2N_2O_3PRe$	$C_{37}H_{34}Br_2N_2O_4PRe$	$C_{35}H_{28}Cl_2N_2O_2PRe$	$C_{35}H_{28}Br_2N_2O_2PRe$
Formula weight	826.69	997.72	796.66	885.58	826.69	947.65	796.66	885.58
T (K)	293.0(2)	293.0(2)	293.0(2)	298.0(1)	293.0(2)	293.0(2)	293.0(2)	298.0(1)
λ (Å)	0.71073	0.71073	0.71073	0.71073	0.71073	0.71073	0.71073	0.71073
Crystal system	monoclinic	monoclinic	monoclinic	monoclinic	monoclinic	monoclinic	triclinic	triclinic
Space group	$P2_1/n$	$C2/c$	$P2_1$	$P2_1$	$P2_1/n$	$P2_1/c$	$P\bar{1}$	$P\bar{1}$
Unit cell dimensions								
a (Å)	9.8196(3)	37.1104(5)	9.2754(4)	9.3436(5)	9.9530(4)	9.9416(4)	7.9061(4)	8.0690(3)
b (Å)	22.2897(7)	15.2308(6)	17.1246(6)	17.1874(6)	20.4722(9)	20.5902(9)	11.7360(6)	11.7247(4)
c (Å)	14.8141(4)	14.6871(12)	10.4910(4)	10.5612(6)	17.3166(8)	17.8865(12)	17.8939(10)	17.6547(5)
α (°)							92.530(5)	91.703(3)
β (°)	91.064(2)	106.587(3)	110.856(5)	110.906(6)	105.233(4)	105.971(6)	91.168(5)	90.309(3)
γ (°)							105.156(5)	104.982(3)
V (Å^3)	3241.88(17)	7956.0(7)	1557.17(10)	1584.38(14)	3404.5(3)	3520.0(3)	1600.10(15)	1612.60(9)
Z	4	8	2	2	4	4	2	2
D_{calc}(mg/m^3)	1.694	1.666	1.699	1.856	1.613	1.788	1.654	1.824
Absorption coefficient (mm^{-1})	4.002	5.145	4.160	6.442	3.811	5.810	4.049	6.329
$F(000)$	1632	3904	784	856	1632	1848	784	856
Crystal size (mm)	0.102 × 0.131 × 0.204	0.324 × 0.162 × 0.016	0.007 × 0.126 × 0.154	0.069 × 0.089 × 0.147	0.025 × 0.106 × 0.248	0.154 × 0.071 × 0.019	0.082 × 0.055 × 0.031	0.029 × 0.048 × 0.290
θ range for data collection (°)	3.30–25.00	3.38–25.00	3.34–25.00	3.45–25.00	3.42–25.00	3.60–25.00	3.42–25.00	3.46–25.00
Index ranges	$-11 \leqslant h \leqslant 11$, $-26 \leqslant k \leqslant 26$, $-16 \leqslant l \leqslant 17$	$-43 \leqslant h \leqslant 44$, $-18 \leqslant k \leqslant 14$, $-17 \leqslant l \leqslant 17$	$-11 \leqslant h \leqslant 11$, $-20 \leqslant k \leqslant 20$, $-12 \leqslant l \leqslant 12$	$-10 \leqslant h \leqslant 11$, $-20 \leqslant k \leqslant 20$, $-9 \leqslant l \leqslant 12$	$-11 \leqslant h \leqslant 11$, $-15 \leqslant k \leqslant 24$, $-17 \leqslant l \leqslant 20$	$-9 \leqslant h \leqslant 11$, $-24 \leqslant k \leqslant 21$, $-21 \leqslant l \leqslant 17$	$-9 \leqslant h \leqslant 9$, $-13 \leqslant k \leqslant 13$, $-21 \leqslant l \leqslant 21$	$-9 \leqslant h < \leqslant 9$, $-13 \leqslant k \leqslant 13$, $-20 \leqslant l \leqslant 20$
Reflections collected	19405	20402	10907	7919	19116	11373	12799	14375
Independent reflections (R_{int})	5688 (0.0357)	6984 (0.0897)	5307 (0.0389)	5315 (0.0293)	5971 (0.0402)	5888 (0.0394)	5616 (0.1109)	5663 (0.0526)
Completeness to $2\theta = 50°$ (%)	99.7	99.7	99.7	99.7	99.7	94.9	99.6	99.8
Maximum and minimum transmission	0.402 and 1.000	0.238 and 1.000	0.503 and 1.000	0.580 and 1.000	0.638 and 1.000	0.628 and 1.000	0.512 and 1.000	0.305 and 1.000
Data/restraints/parameters	5688/0/408	6984/0/464	5307/1/389	5315//1/389	5971/0/408	5888/0/428	5616/0/389	5663/0/389
Goodness-of-fit (GOF) on F^2	1.030	0.985	0.993	1.114	1.056	1.009	1.062	0.992
Final R indices [$I > 2\sigma(I)$]	$R_1 = 0.0243$, $wR_2 = 0.0482$	$R_1 = 0.0670$, $wR_2 = 0.1657$	$R_1 = 0.0300$, $wR_2 = 0.0493$	$R_1 = 0.0325$, $wR_2 = 0.0728$	$R_1 = 0.0327$, $wR_2 = 0.0748$	$R_1 = 0.0343$, $wR_2 = 0.0688$	$R_1 = 0.0507$, $wR_2 = 0.0810$	$R_1 = 0.0360$, $wR_2 = 0.0720$
R indices (all data)	$R_1 = 0.0339$, $wR_2 = 0.0506$	$R_1 = 0.0941$, $wR_2 = 0.1858$	$R_1 = 0.0393$, $wR_2 = 0.0513$	$R_1 = 0.0384$, $wR_2 = 0.0864$	$R_1 = 0.0495$, $wR_2 = 0.0820$	$R_1 = 0.0568$, $wR_2 = 0.0751$	$R_1 = 0.0844$, $wR_2 = 0.0867$	$R_1 = 0.0467$, $wR_2 = 0.0756$
Largest different peak and hole (e Å^{-3})	0.638 and −0.504	4.260 and −1.712	0.643 and −0.599	1.094 and −0.564	1.273 and −0.834	0.912 and −0.541	1.712 and −1.399	1.797 and −1.080

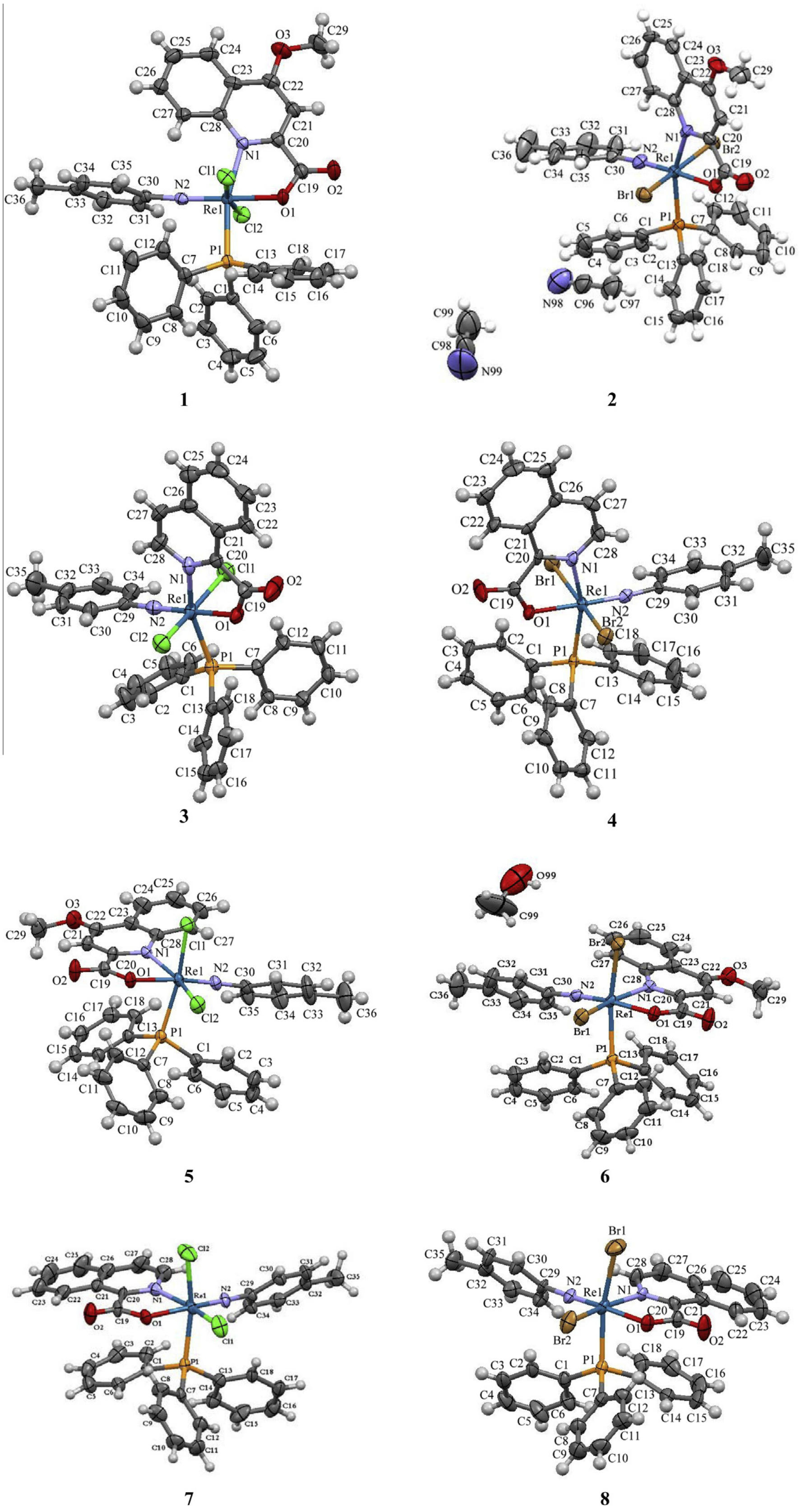

1 2 3 4 5 6 7 8

Fig. 1. The molecular structures of **1–8**. Displacement ellipsoids are drawn at 50% probability.

Please cite this article in press as: I. Gryca et al., Inorg. Chim. Acta (2016), http://dx.doi.org/10.1016/j.ica.2016.04.030

Table 2
The experimental bond lengths (Å) and angles (°) for **1**–**8**.

	1 (X = Cl)	**2** (X = Br)	**3** (X = Cl)	**4** (X = Br)	**5** (X = Cl)	**6** (X = Br)	**7** (X = Cl)	**8** (X = Br)
Bond lengths								
Re(1)—N(2)	1.712(3)	1.726(7)	1.703(5)	1.712(8)	1.707(4)	1.718(4)	1.711(5)	1.700(4)
Re(1)—O(1)	2.050(2)	2.029(6)	2.045(4)	2.044(6)	2.054(3)	2.051(3)	2.055(4)	2.044(3)
Re(1)—N(1)	2.184(3)	2.195(7)	2.134(5)	2.120(8)	2.169(4)	2.173(4)	2.108(6)	2.105(4)
Re(1)—X(1)	2.3897(9)	2.427(2)	2.3971(16)	2.5455(10)	2.3679(12)	2.5200(6)	2.370(2)	2.5131(6)
Re(1)—X(2)	2.4045(9)	2.5514(10)	2.4134(17)	2.5632(10)	2.3976(13)	2.5467(7)	2.401(2)	2.5507(6)
Re(1)—P(1)	2.4205(9)	2.5523(10)	2.4332(16)	2.428(2)	2.4464(13)	2.4541(15)	2.4514(18)	2.4574(13)
Bond angles								
N(2)—Re(1)—O(1)	173.38(11)	176.1(3)	178.2(2)	178.0(3)	170.39(17)	169.73(18)	167.3(2)	168.40(16)
N(2)—Re(1)—N(1)	101.37(11)	108.3(3)	105.7(2)	104.0(3)	100.67(16)	100.47(17)	95.1(2)	96.15(17)
O(1)—Re(1)—N(1)	74.81(10)	75.6(2)	74.62(17)	75.2(3)	74.53(12)	74.64(13)	74.32(19)	74.75(14)
N(2)—Re(1)—X(1)	99.02(9)	94.3(2)	95.82(16)	94.2(2)	98.57(14)	97.94(14)	100.24(19)	98.24(13)
O(1)—Re(1)—X(1)	86.38(8)	86.20(17)	86.02(12)	87.52(18)	86.92(9)	87.75(9)	90.83(14)	91.37(9)
N(1)—Re(1)—X(1)	88.31(7)	85.79(19)	84.33(13)	84.1(2)	160.43(10)	161.22(11)	164.36(15)	165.20(10)
N(2)—Re(1)—X(2)	92.36(9)	94.5(2)	92.22(16)	91.7(2)	99.69(14)	100.39(15)	99.25(19)	98.90(13)
O(1)—Re(1)—X(2)	81.92(8)	85.62(17)	85.98(13)	86.42(18)	88.26(10)	88.19(11)	86.97(14)	87.40(10)
N(1)—Re(1)—X(2)	84.05(7)	83.21(19)	85.70(14)	85.8(2)	84.57(10)	84.04(11)	84.69(16)	83.77(11)
X(1)—Re(1)—X(2)	167.36(3)	167.64(4)	168.58(6)	69.30(4)	88.75(5)	89.05(2)	89.73(9)	90.60(2)
N(2)—Re(1)—P(1)	93.45(9)	93.5(2)	93.13(16)	93.9(2)	90.59(14)	90.86(15)	93.35(19)	93.17(14)
O(1)—Re(1)—P(1)	90.34(7)	82.64(18)	86.60(11)	86.86(18)	81.68(10)	80.82(11)	80.62(13)	80.48(10)
N(1)—Re(1)—P(1)	165.14(7)	158.19(19)	161.22(13)	162.1(2)	95.38(10)	95.97(12)	94.01(15)	93.69(11)
X(1)—Re(1)—P(1)	90.37(3)	90.85(6)	94.20(5)	95.21(6)	87.91(5)	87.41(4)	88.25(7)	88.95(3)
X(2)—Re(1)—P(1)	94.44(3)	97.28(6)	93.45(5)	93.26(6)	169.56(4)	168.57(4)	167.39(6)	167.85(4)
C(30)—N(2)—Re(1)	171.2(2)	176.0(7)	176.5(4) C(29)	174.2(6) C(29)	177.0(4)	176.6(4)	177.5(5) C(29)	177.9(4) C(29)

π orbitals of phosphine ligand and p chloride orbitals and contains only small amount of $\pi_{\mathrm{Re}\equiv\mathrm{NR}}$ orbital. The H-2 of **1**, **3**, **5** and **7** is mostly contributed by orbitals of the chelating ligand, whereas the other high-lying occupied molecular orbitals are predominately localized on PPh_3 ligand. The LUMO, LUMO + 1 and LUMO + 2 are delocalized on the rhenium atom (d_{xz} and d_{yz} orbitals) and π-antibonding orbitals of the imido and carboxylate ligands. The d_{yz} and d_{xy} rhenium orbitals bear antibonding character towards the p_π nitrogen orbitals of the imido ligand. To a large extent, these molecular orbitals can be considered as $\pi^*_{\mathrm{Re}\equiv\mathrm{NR}}$ orbitals.

In order to assign UV–Vis absorption bands and better understand the spectroscopic characteristics of the complexes **1**, **3**, **5** and **7**, TDDFT calculations have been carried out. The experimental and calculated electronic spectra of **1**–**4** are compared in Fig. S3. Tables S8–S11 present the most important electronic transitions calculated with the TDDFT method assigned to the observed absorption bands of **1**, **3**, **5** and **7**, respectively.

The low-energy absorption bands, observed at 818, 615 and 448 nm for **1**, 759, 606 and 460 nm for **3**, 668 and 457 nm for **5** and 685, 576 and 464 nm for **7**, are contributed by transitions d/π(Cl)/π(L)→d/π*(L)/π*(*p*-tol) for **1**, **5** and **7** and d/π(Cl)→d/π*(*p*-tol)/π*(L) for **3**. They can be seen as mixed d→d (*Ligand Field; LF*), π(L)/π(X)→d (*Ligand–Metal Charge Transfer*; *LMCT*), d→π*(L) (*Metal–Ligand Charge Transfer*; *MLCT*) and π(L)→π*(L) (*Ligand–Ligand Charge Transfer*; *LLCT*) or a delocalized *MLLCT* (metal–ligand-to-ligand CT) character can be assigned as the origin for these transitions. The intense bands in high energy region of **1**, **3**, **5** and **7** are largely attributed to ligand–metal charge transfer (*LMCT*), ligand–ligand charge transfer (*LLCT*) and intraligand transitions (*IL*).

2.5. A study of catalytic activity in oxidations with peroxides

We checked the catalytic activity of prepared rhenium complexes in oxidation of organic compounds with peroxides. The complexes turned out to be inactive in oxidation of alkanes and alcohols with hydrogen peroxide.

Some parameters obtained in the oxidation of *n*-heptane with *tert*-butyl hydroperoxide (TBHP) are collected in Table 3 and Fig. 3. Chromatograms of selected experiments are shown in Fig. S4. The oxidation with TBHP catalyzed by the rhenium complexes of *cis*-1,2-dimethylcyclohexane proceeds non-stereoselectively. Thus, parameter *trans*/*cis* for the oxidation catalyzed by **2** was 0.8 that is close to unity. Thus, we can conclude that selectivity parameters testify that alkanes are oxidized by the systems under discussion with the participation of *tert*-butoxy radicals. The oxidation of C—H bonds with TBHP involves the interaction of the alkane with *tert*-butoxy radical *tert*-BuO·. It is noteworthy that the regioselectivity parameter for the oxidation catalyzed by complexes **2**–**6** is similar to that found by us previously in the reaction with the systems containing a strongly hindered reaction center. These catalytic systems are, particularly, the tetracopper(II) triethanolaminate complex $[O\subset Cu_4\{N(CH_2CH_2O)_3\}_4(BOH)_4][BF_4]_2$/TBHP and dinuclear manganese complex $[Mn_2(R\text{-}LMe^{2R})_2(\mu\text{-}O)_2]^{3+}(PF_6)_3$ (where LMe^{2R} is 1-(2-hydroxypropyl)-4,7-dimethyl-1,4,7-triazacyclononane)/oxalic acid/TBHP are shown in Fig. 3. It can be clearly seen that in rhenium-catalyzed oxidations reactivity of C—H bonds in position C(2) is two times higher in comparison with the analogous value for position C(4). It is noteworthy that the chromatograms of reaction mixtures obtained in the oxidation of methylcyclohexane (MCH) testify that a strong shielding of positions 2 of the cyclohexane ring takes place (Fig. S5).

The synthesized rhenium complexes did not exhibit high catalytic activity in oxidation of 1-phenylethanol with TBHP in acetonitrile. The initial rates for the most active complexes are collected in Table S12.

3. Conclusions

Complexes *trans*-(X,X)-$[Re(p\text{-}NC_6H_4CH_3)X_2(N\text{-}O)(PPh_3)_2]$ and *cis*-(X,X)-$[Re(p\text{-}NC_6H_4CH_3)X_2(N\text{-}O)(PPh_3)_2]$ incorporating quinoline or isoquinoline carboxylate bidentate ligands (N—O) were synthesized, characterized and checked as catalysts in oxidations of alkanes and 1-phenylethanol. Formation of isomeric forms (*trans*–*cis*) of $[Re(p\text{-}NC_6H_4CH_3)X_2(4\text{-}MeO\text{-}quin\text{-}2\text{-}COO)(PPh_3)]$ and $[Re(p\text{-}NC_6H_4CH_3)Cl_2(isoquin\text{-}1\text{-}COO)(PPh_3)]$ were found to be solvent-dependent.

Please cite this article in press as: I. Gryca et al., Inorg. Chim. Acta (2016), http://dx.doi.org/10.1016/j.ica.2016.04.030

Molecular orbitals of 1

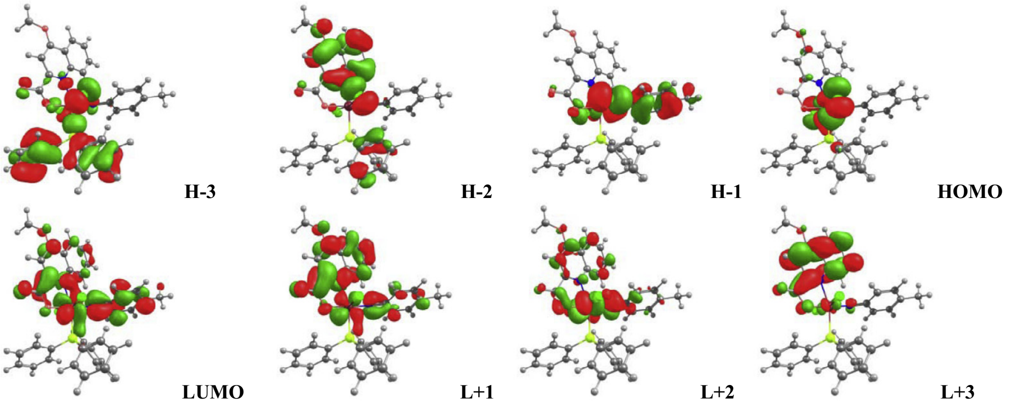

Molecular orbitals of 3

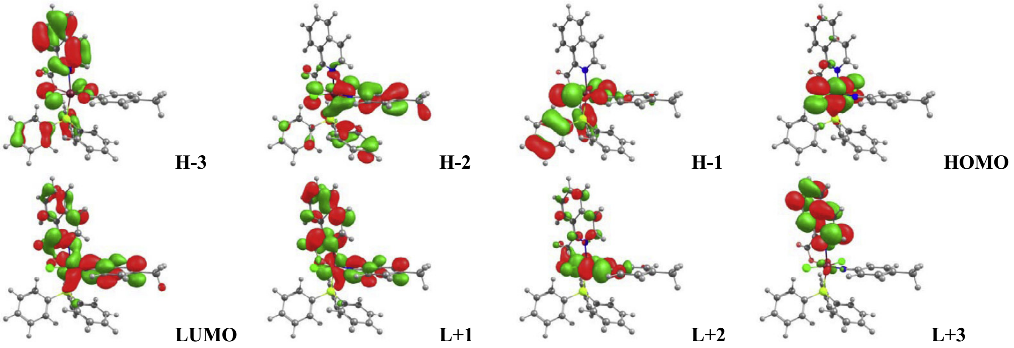

Molecular orbitals of 5

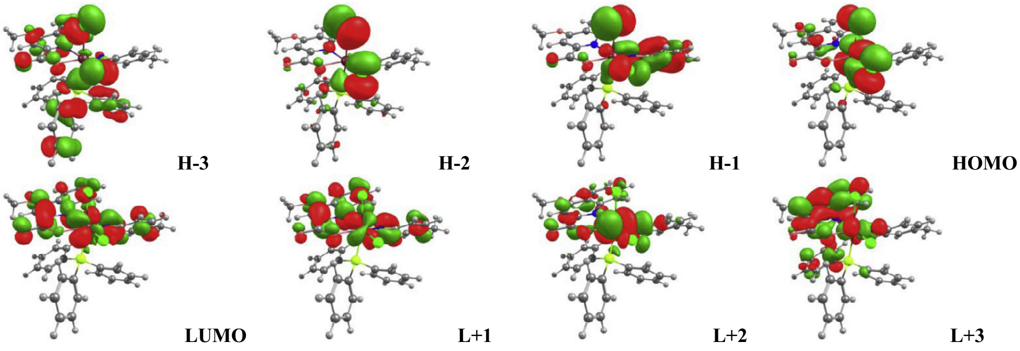

Molecular orbitals of 7

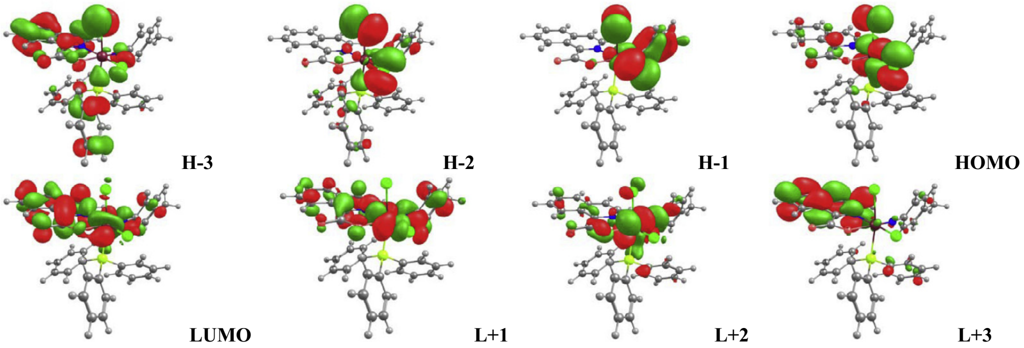

Fig. 2. The contours of the selected frontier orbitals of **1**, **3**, **5** and **7**.

Table 3
Oxidation of *n*-heptane catalyzed by certain rhenium complexes prepared in the present work.[a]

Entry	Catalyst	TON	Parameter C(2):C(3):C(4)
1	**2**	10	1.0:0.57:0.48
2	**3**	11	1.0:0.57:0.43
3	**4**	16	1.0:0.60:0.44
4	**5**	12	1.0:0.68:0.46
5	**6**	14	1.0:0.55:0.45

[a] Conditions. Catalyst, 2×10^{-4} M; TBHP (70% aqueous), 0.45 M, HNO_3, 0.05 M; 2 h, 60 °C. Concentration of isomeric heptanoles present in the reaction solution was measured after reduction of a sample with PPh_3 (see Fig. S4). The TON is number of moles of product produced per one mol of catalyst. Parameters C(1):C(2):C(3):C(4) are relative normalized reactivities of H atoms at carbon atoms C(1), C(2), C(3) and C(4) of *n*-heptane or *n*-octane chain.

The findings enhance our understanding of the structural preferences of the imido rhenium(V) complexes with uninegative N,O-donor ligands. The X-ray studies and NBO analysis confirm a linear coordination mode of the *p*-$NC_6H_4CH_3$ ligand and triple bond between the rhenium and the imido ligand. The results clearly indicate that the molecular structure of [Re(*p*-$NC_6H_4CH_3$)X_2(N-O)(PPh_3)$_2$] compounds is predominantly governed by multiply bonded imido ligand, and their isomeric preferences are controlled kinetically rather than thermodynamically. Some complexes exhibited a moderate activity in regioselective oxidations with TBHP.

4. Experimental

4.1. Materials

The reagents used to the synthesis were commercially available and they were used without further purification. The complexes *mer*-[Re(*p*-$NC_6H_4CH_3$)X_3(PPh_3)$_2$] (X = Cl, Br) and *trans*-[Re(*p*-$NC_6H_4CH_3$)X_2(OMe)(PPh_3)$_2$] (X = Cl, Br) were prepared according to the literature methods [7f,14].

4.2. Physical measurements

Infrared spectra were recorded on a Nicolet iS5 spectrophotometer in the spectral range 4000–400 cm^{-1} with the samples in the form of potassium bromide pellets. Electronic spectra were measured on a spectrophotometer Lab Alliance UV–VIS 8500 in the range 1100÷190 nm in acetonitrile solution. The ^1H NMR, ^{13}C NMR and ^{31}P NMR spectra were recorded (298 K) on Bruker Advance 500 NMR spectrometer at a resonance frequency of 500 MHz for ^1H NMR spectra, 125 MHz for ^{13}C NMR spectra and

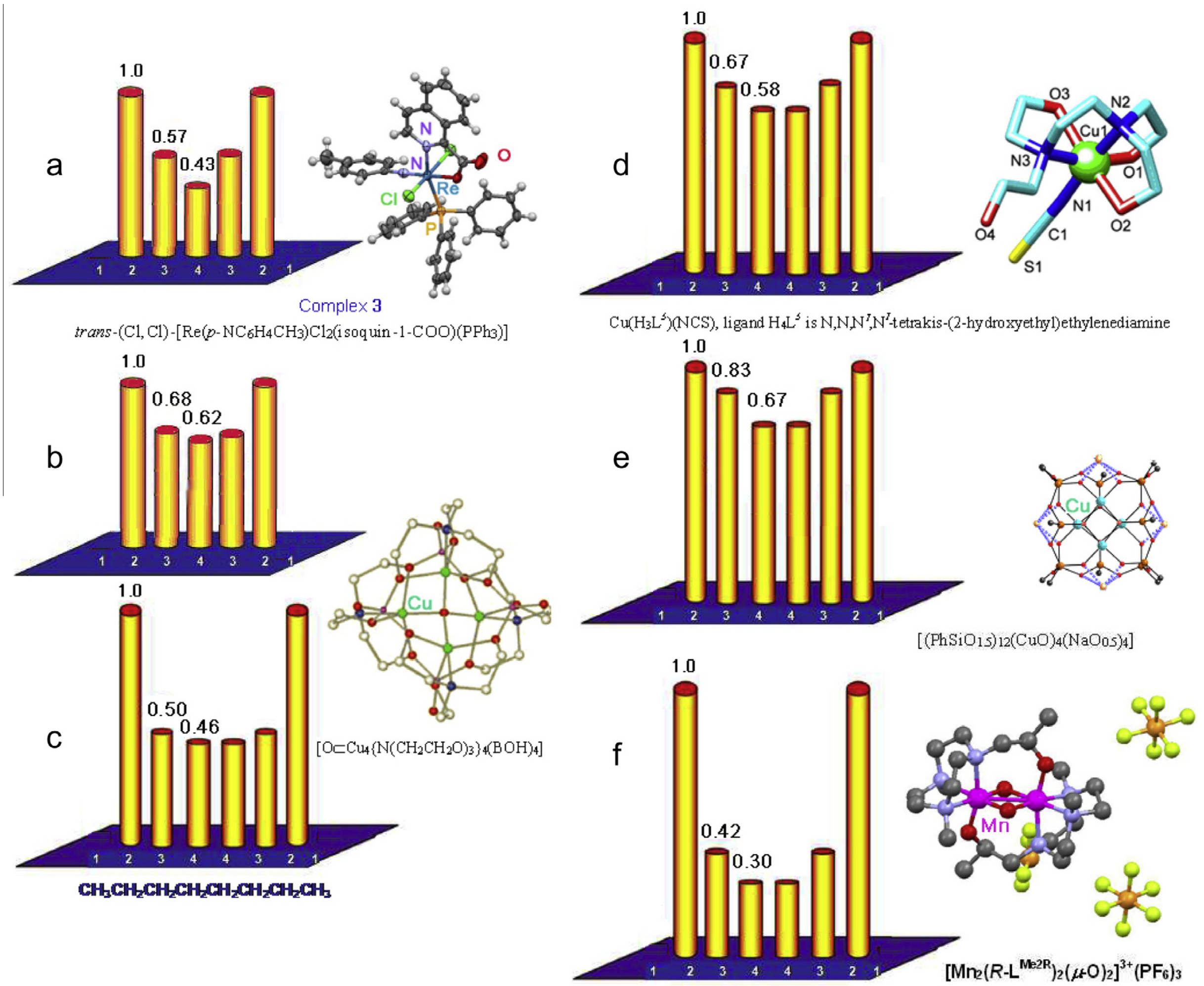

Fig. 3. Regioselectivity profiles for the oxidation of *n*-heptane (a and b) and *n*-octane (c–f) with TBHP catalyzed by various metal complexes: *trans*-(Cl,Cl)-[Re(*p*-$NC_6H_4CH_3$)Cl_2(isoquin-1-COO)(PPh_3)] (complex **3**; this work) (a); tetracopper(II) triethanolaminate complex [O⊂Cu_4{N(CH_2CH_2O)$_3$}$_4$(BOH)$_4$][BF_4]$_2$.(Ref. [13a]): reaction with *n*-heptane (b) and *n*-octane (c); Cu(H_3L^3)(NCS) where ligand H_4L^3 is N,N,N′,N′-tetrakis-(2-hydroxyethyl)ethylenediamine (Ref. [13b]) (d); [($PhSiO_{1.5}$)$_{12}$(CuO)$_4$($NaO_{0.5}$)$_4$] (Ref. [13c]) (e); [Mn_2(*R*-LMe^{2R})$_2$(μ-O)$_2$]$^{3+}$(PF_6)$_3$, where LMe^{2R} is 1-(2-hydroxypropyl)-4,7-dimethyl-1,4,7-triazacyclononane (Ref. [13d]) (f).

Please cite this article in press as: I. Gryca et al., Inorg. Chim. Acta (2016), http://dx.doi.org/10.1016/j.ica.2016.04.030

162 MHz for ^{31}P NMR using DMSO-d_6 as solvent and TMS as an internal standard. Elemental analyses (C, H, N) were performed on a Perkin-Elmer CHN-2400 analyser.

4.3. Preparation of complexes **1–4**

Starting complex *mer*-[Re(*p*-$NC_6H_4CH_3$)X_3(PPh_3)$_2$] (0.54 mmol) was added to the corresponding N-heterocyclic carboxylic acid (0.60 mmol) in acetonitrile (60 mL) and the reaction mixture was refluxed for 6 h. The resulting solution was reduced in volume to 10 mL and allowed to cool to room temperature. A crystalline precipitate of **1**–**4** was filtered off and dried in the air. X-ray quality brown crystals of **1**–**4** were obtained by slow recrystallization from acetonitrile.

4.3.1. *trans-(Cl,Cl)-[Re(p-$NC_6H_4CH_3$)Cl_2(4-MeO-quin-2-COO)(PPh_3)] (**1**)*

[Re(*p*-$NC_6H_4CH_3$)Cl_3(PPh_3)$_2$] (0.48 g) and 4-methoxy-2-quinolinecarboxylic acid (0.12 g) yielded 357 mg of complex **1**; yield 80%. $C_{36}H_{30}Cl_2N_2O_3PRe$ (826.69 g/mol): Calc. C, 53.30; H, 3.66; N, 3.39; found: C, 52.83; H, 3.64; N, 3.38%.

IR (KBr; ν/cm^{-1}): 3050(w), 1686(vs), 1586(s), 1518(m), 1482 (w), 1434(m), 1386(w), 1366(s), 1351(sh), 1328(m), 1301(w), 1285(w), 1274(w), 1258(w), 1229(w), 1171(w), 1122(m), 1101 (sh), 1092(w), 1032(w), 1015(w), 998(m), 960(w), 898(w), 855 (w), 827(w), 804(w), 790(w), 769(m), 748(m), 706(sh), 693(m), 647(w), 619(w), 574(w), 530(s), 503(m) and 445(w).

^{1}H NMR (400 MHz, DMSO-d_6, ppm): δ = 8.29 (d, 1H, 10.0 Hz), 8.12 (d, 1H, 7.8 Hz), 7.77 (t, 1H, 7.6 Hz), 7.69 (s, 1H), 7.65–7.57 (m, 6H), 7.50 (d, 10H, 6.3 Hz), 7.44 (d, 2H, 8.1 Hz), 7.13 (d, 2H, 8.1 Hz), 4.32 (s, 3H) and 2.21 (s, 3H).

^{13}C NMR (125 MHz, DMSO-d_6): δ = 166.9, 166.1, 155.9, 148.4, 145.3, 143.6, 143.1, 141.7, 139.2, 138.6, 136.6, 134.7, 132.0, 131.8, 131.7, 131.1, 129.8, 129.3, 128.8, 126.7, 124.7, 123.5, 122.0, 121.9, 102.2, 58.1, 22.2 ppm.

^{31}P NMR (DMSO-d_6): δ = 25.69 ppm.

UV–Vis (MeCN; λ_{max} [nm] (ε; [dm^3 mol^{-1} cm^{-1}])): 818 (114); 615 (146); 448 (611); 411 (640); 324 (6237); 298 (5709); 232 (29 497).

4.3.2. *trans-(Br,Br)-[Re(p-$NC_6H_4CH_3$)Br_2(4-MeO-quin-2-COO)(PPh_3)]·2MeCN (**2**)*

[Re(*p*-$NC_6H_4CH_3$)Br_3(PPh_3)$_2$] (0.52 g) and 4-methoxy-2-quinolinecarboxylic acid (0.12 g) yielded 430 mg of **2**; yield 80%. $C_{40}H_{36}Br_2N_4O_3PRe$ (997.72 g/mol): Calc. C, 48.15; H, 3.64; N, 5.61; found: C, 49.13; H, 3.66; N, 5.55%.

IR (KBr; ν/cm^{-1}): 3051(w), 1698(vs), 1588(s), 1519(w), 1482 (w), 1458(w), 1435(m), 1391(m), 1365(s), 1329(m), 1274(sh), 1257(w), 1227(w), 1185(w), 1171(w), 1155(w), 1132(sh), 1115 (m), 1091(w), 1031(w), 1019(w), 996(w), 889(w), 861(w), 827 (sh), 815(sh), 804(w), 790(w), 768(w), 753(w), 746(w), 694(m), 618(w), 565(w), 529(s), 511(w), 494(w) and 456(w).

^{1}H NMR (400 MHz, DMSO-d_6, ppm): δ = 8.32 (d, 1H, 8.1 Hz), 8.06 (d, 1H, 8.7 Hz), 7.78 (t, 1H, 7.7 Hz), 7.71–7.59 (m, 8H), 7.50 (d, 11H, 8.0 Hz), 7.15 (d, 2H, 8.1 Hz), 4.32 (s, 3H), 2.24 (s, 3H) and 2.07(s, 6H).

^{13}C NMR (125 MHz, DMSO-d_6): δ = 167.3, 163.7, 147.9, 142.9, 133.9, 133.5, 132.7, 132.6, 132.5, 131.9, 130.7, 129.4, 129.3, 129.2, 125.3, 123.5, 122.8, 121.6, 118.6, 101.8, 58.4, 20.88 and 1.62 ppm.

^{31}P NMR (DMSO-d_6): δ = 25.64 ppm.

UV–Vis (MeCN; λ_{max} [nm] (ε; [dm^3 mol^{-1} cm^{-1}])): 765 (263); 620 (397); 462 (1517); 422 (2337); 328 (21 693); 300 (22 741); 199 (217 102).

4.3.3. *trans-(Cl,Cl)-[Re(p-$NC_6H_4CH_3$)Cl_2(isoquin-1-COO)(PPh_3)] (**3**)*

[Re(*p*-$NC_6H_4CH_3$)Cl_3(PPh_3)$_2$] (0.48 g) and isoquinoline-1-carboxylic acid (0.10 g) yielded 322 mg of **3**; yield 75%. $C_{35}H_{28}Cl_2N_2O_2PRe$ (796.66 g/mol): Calc. C, 52.77; H, 3.54; N, 3.52; found: C, 52.85; H, 3.51; N, 3.48%.

IR (KBr; ν/cm^{-1}): 3058(w), 1684(vs), 1617(w), 1589(w), 1560 (w), 1482(w), 1449(w), 1436(m), 1359(w), 1322(w), 1313(w), 1278(m), 1246(s), 1209(w), 1185(w), 1167(sh), 1154(m), 1142 (sh), 1097(w), 1089(w), 1014(w), 1005(w), 997(w), 886(w), 829 (m), 817(sh), 799(w), 760(w), 751(w), 742(w), 701(sh), 691(s), 670(w), 618(w), 568(w), 525(s), 511(m), 501(m), 448(w) and 428 (w).

^{1}H NMR (400 MHz, DMSO-d_6, ppm): δ = 8.37 (d, 1H, 6.3 Hz), 8.27 (d, 1H, 8.1 Hz), 8.03 (t, 1H, 7.8 Hz), 7.91 (t, 2H, 8.0 Hz), 7.66–7.58 (m, 6H), 7.49 (dd, 12H, 14.9, 6.8 Hz), 7.28 (d, 2H, 8.1 Hz) and 2.29 (s, 3H).

^{13}C NMR (125 MHz, DMSO-d_6): δ = 164.8, 159.8, 156.0, 155.0, 154.1, 144.7, 142.0, 140.3, 139.3, 134.6, 134.5, 131.7, 131.6, 131.1, 128.9, 128.8, 127.9, 127.7, 126.4, 124.2, 122.3, 122.0, 121.4 and 22.3 ppm.

^{31}P NMR (DMSO-d_6): δ = 25.55 ppm.

UV–Vis (MeCN; λ_{max} [nm] (ε; [dm^3 mol^{-1} cm^{-1}])): 759 (165); 606 (801); 460 (5680); 326 (22 616); 235 (101 216); 199 (184 009).

4.3.4. *trans-(Br,Br)-[Re(p-$NC_6H_4CH_3$)Br_2(isoquin-1-COO)(PPh_3)] (**4**)*

[Re(*p*-$NC_6H_4CH_3$)Br_3(PPh_3)$_2$] (0.52 g) and isoquinoline-1-carboxylic acid (0.10 g) yielded 360 mg of **4**; yield 75%. $C_{35}H_{28}Br_2N_2O_2PRe$ (885.58 g/mol): Calc. C, 47.47; H, 3.19; N, 3.16, found: C, 46.83; H, 3.10; N, 3.25%.

IR (KBr; ν/cm^{-1}): 3059(w), 1685(vs), 1640(sh), 1617(sh), 1590 (w), 1482(w), 1436(m), 1358(w), 1278(m), 1246(s), 1210(sh), 1186(w), 1167(sh), 1154(m), 1142(sh), 1096(w), 1089(sh), 1014 (w), 997(w), 887(w), 829(m), 818(sh), 799(w), 760(w), 751(w), 742(w), 691(s), 670(sh), 568(w), 525(s), 511(m), 500(sh), 488(sh), 455(w), 448(w), 420(w).

^{1}H NMR (400 MHz, DMSO-d_6, ppm): δ = 9.50 (d, 1H, 8.9 Hz), 8.38 (d, 1H, 6.1 Hz), 8.26 (d, 1H, 8.4 Hz), 8.06–7.99 (m, 1H), 7.92 (d, 2H, 6.5 Hz), 7.71–7.61 (m, 6H), 7.56 (d, 2H, 8.0 Hz), 7.50 (s, 9H), 7.29 (d, 2H, 7.8 Hz) and 2.30 (s, 3H).

^{13}C NMR (125 MHz, DMSO-d_6): δ = 167.1, 154.2, 142.5, 142.3, 141.5, 140.4, 140.1, 139.6, 138.9, 134.7, 134.0, 133.6, 131.9, 131.6, 131.4, 131.2, 130.0, 129.5, 129.3, 129.0, 128.9, 128.7, 128.2, 127.7, 127.6, 126.3, 124.6, 124.1, 121.9 and 22.5 ppm.

^{31}P NMR (DMSO-d_6): δ = 25.81 ppm.

UV–Vis (MeCN; λ_{max} [nm] (ε; [dm^3 mol^{-1} cm^{-1}])): 752 (238); 605 (1087); 461 (15 708); 321 (57 025); 278 (56 757); 234 (174 820); 197 (303 334).

4.4. Preparation of complexes **5–8**

Complex *trans*-(X,X)-[Re(*p*-$NC_6H_4CH_3$)X_2(OMe)(PPh_3)$_2$] (0.54 mmol) was added to the corresponding N-heterocyclic carboxylic acid (0.60 mmol) in methanol (60 mL) and the reaction mixture was refluxed for 6 h. The resulting solution was reduced in volume to 10 mL and allowed to cool to room temperature. A crystalline precipitate of mixture of **5**–**8** was filtered off and dried in the air. The mixture of X-ray quality green crystals of **5**–**8** was obtained by slow recrystallization from methanol.

4.4.1. *cis-(Cl,Cl)-[Re(p-$NC_6H_4CH_3$)Cl_2(4-MeO-quin-2-COO)(PPh_3)] (**5**)*

[Re(*p*-$NC_6H_4CH_3$)Cl_3(PPh_3)$_2$] (0.48 g) and 4-methoxy-2-quinolinecarboxylic acid (0.12 g) yielded 357 mg of product; yield 80%. The crystals of **1** and **5** were manually separated using a microscope and they were collected in 45% and 35% yield, respectively. $C_{36}H_{30}Cl_2N_2O_3PRe$ (826.69 g/mol): Calc. C, 52.30; H, 3.66; N, 3.39; found: C, 52.61; H, 3.15; N, 3.57%.

IR (KBr; ν/cm^{-1}): 3054(w), 1686(vs), 1616(w), 1589(s), 1561 (sh), 1521(w), 1481(w), 1461(w), 1433(w), 1392(m), 1364(s), 1330(w), 1262(w), 1189(w), 1173(w), 1164(w), 1131(sh), 1117 (m), 1093(w), 1021(w), 996(w), 953(w), 888(w), 859(w), 804(w), 791(w), 756(w), 692(w), 528(m), 501(w) and 447(w).

^{1}H NMR (400 MHz, DMSO-d_6, ppm): δ = 8.35 (d, 1H, 8.3 Hz), 7.96 (d, 1H, 8.9 Hz), 7.82(t, 1H, 7.6 Hz), 7.66–7.85 (m, 1H), 7.29–7.19 (m, 6H), 7.19–7.11 (m, 9H), 7.05 (d, 2H, 8.3 Hz), 6.99 (d, 2H, 8.4 Hz), 6.95 (s, 1H), 4.14 (s, 3H), 2.23 (s, 3H).

^{13}C NMR (125 MHz, DMSO-d_6): δ = 168.2, 166.9, 154.1, 149.8, 143.9, 141.8, 134.7, 134.6, 134.1, 134.0, 133.1, 131.7, 131.4, 130.6, 129.8, 129.4, 129.2, 129.0, 128.9, 128.8, 128.8, 128.7, 126.6, 125.7, 123.3, 122.9, 122.1, 101.3, 100.7, 57.9, 57.1, 22.3 ppm.

^{31}P NMR (DMSO-d_6): δ = 25.74 ppm.

UV–Vis (MeCN; λ_{max} [nm] (ε; [dm^3 mol^{-1} cm^{-1}])): 668 (278); 457 (3422); 330 (13924); 305 (13294); 234 (57933); 190 (130151).

4.4.2. cis-(Br,Br)-[Re(p-NC$_6$H$_4$CH$_3$)Br$_2$(4-MeO-quin-2-COO)(PPh$_3$)]·MeOH (**6**)

[Re(p-NC$_6$H$_4$CH$_3$)Br$_3$(PPh$_3$)$_2$] (0.52 g) and 4-methoxy-2-quinolinecarboxylic acid (0.12 g) yielded 430 mg of product; yield 80%. The crystals of **2** and **6** were manually separated using a microscope and they were collected in 45% and 35% yield, respectively. $C_{37}H_{34}Br_2N_2O_4PRe$ (947.65 g/mol): Calc. C, 46.90; H, 3.62; N, 2.96; found: C, 47.11; H, 3.59; N, 2.95%.

IR (KBr; ν/cm^{-1}): 3049(w), 1686(vs), 1587(s), 1518(m), 1481 (w), 1453(w), 1433(m), 1386(w), 1365(s), 1329(m), 1302(w), 1283(w), 1257(w), 1186(sh), 1179(w), 1172(w), 1117(m), 1091 (w), 1033(w), 1015(w), 997(m), 959(w), 952(w), 888(w), 855(w), 827(w), 803(w), 789(w), 768(w), 754(m), 705(sh), 692(m), 647 (w), 619(w), 573(w), 529(s), 501(m), 458(w), 444(w).

^{1}H NMR (400 MHz, DMSO-d_6, ppm): δ = 8.32 (d, 1H, 8.1 Hz), 8.06 (d, 1H, 8.9 Hz), 7.78 (t, 1H, 7.6 Hz), 7.67 (dd, 8H, 16.4, 8.3 Hz), 7.49 (d, 11H, 8.2 Hz), 7.15 (d, 2H, 8.3 Hz), 4.32 (s, 3H), 2.24 (s, 3H), 2.07 (s, 3H).

^{13}C NMR (125 MHz, DMSO-d_6): δ = 164.9, 163.9, 149.1, 144.0, 134.1, 134.0, 133.6, 132.8, 132.5, 131.9, 131.8, 131.4, 130.8, 130.7, 129.7, 129.2, 129.1, 129.0, 128.9, 127.0, 126.4, 125.7, 125.4, 123.3, 122.4, 121.6, 109.9, 101.2, 57.8, 22.3 ppm.

^{31}P NMR (DMSO-d_6): δ = 25.79 ppm.

UV–Vis (MeCN; λ_{max} [nm] (ε; [dm^3 mol^{-1} cm^{-1}])): 666 (81); 557 (128); 462 (2831); 402 (7997); 352 (13138); 289 (17527); 250 (33505); 210 (86171).

4.4.3. cis-(Cl,Cl)-[Re(p-NC$_6$H$_4$CH$_3$)Cl$_2$(isoquin-1-COO)(PPh$_3$)] (**7**)

[Re(p-NC$_6$H$_4$CH$_3$)Cl$_3$(PPh$_3$)$_2$] (0.48 g) and isoquinoline-1-carboxylic acid (0.10 g) yielded 322 mg of product; yield 75%. The crystals of **3** and **7** were manually separated using a microscope and they were collected in 40% and 35% yield, respectively.) $C_{35}H_{28}Cl_2N_2O_2PRe$ (796.66 g/mol): Calc. C, 52.77; H, 3.54; N, 3.52; found: C, 52.85; H, 3.51; N, 3.48%.

IR (KBr; ν/cm^{-1}): 3059(w), 1690(vs), 1654(sh), 1641(sh), 1591 (m), 1551(w), 1481(m), 1434(s), 1356(w), 1320(w), 1275(w), 1241(m), 1187(w), 1169(w), 1155(m), 1141(w), 1096(m), 1015 (w), 999(w), 888(m), 818(m), 799(w), 756(sh), 750(m), 743(sh), 720(sh), 696(s), 673(w), 528(s), 515(m), 495(m), 439(w).

^{1}H NMR (400 MHz, DMSO-d_6, ppm): δ = 9.00 (d, 1H, 8.8 Hz), 8.15 (t, 2H, 7.6 Hz), 7.87–7.82 (m, 2H), 7.73 (t, 1H, 7.6 Hz), 7.42 (ddd, 6H, 10.9, 8.5, 5.2 Hz), 7.22 (dd, 9H, 4.5, 2.5 Hz), 7.17 (d, 2H, 8.2 Hz), 7.07 (d, 2H, 8.4 Hz), 2.26 (s, 3H).

^{13}C NMR (125 MHz, DMSO-d_6): δ = 166.5, 152.8, 150.6, 148.9, 146.1, 143.4, 142.0, 141.4, 141.3, 140.3, 138.8, 137.6, 136.8, 136.2, 135.9, 133.9, 133.8, 133.6, 132.3, 131.5, 131.0, 129.8, 129.5, 129.0, 128.9, 128.8, 127.9, 127.4, 127.4, 126.7, 126.0, 124.8, 122.3, 120.9, 120.0, 22.25 ppm.

^{31}P NMR (DMSO-d_6): δ = 25.42 ppm.

UV–Vis (MeCN; λ_{max} [nm] (ε; [dm^3 mol^{-1} cm^{-1}])): 685 (167); 576 (277); 464 (2660); 353 (5688); 317 (21199); 279 (58217); 240 (71837); 191 (127721).

4.4.4. cis-(Br,Br)-[Re(p-NC$_6$H$_4$CH$_3$)Br$_2$(isoquin-1-COO)(PPh$_3$)] (**8**)

[Re(p-NC$_6$H$_4$CH$_3$)Br$_3$(PPh$_3$)$_2$] (0.52 g) and isoquinoline-1-carboxylic acid (0.10 g) yielded 360 mg of product; yield 75%. The crystals of **4** and **8** were manually separated using a microscope and they were collected in 40% and 35% yield, respectively. $C_{35}H_{28}Br_2N_2O_2PRe$ (885.58 g/mol): Calc. C, 47.47; H, 3.19; N, 3.16; found: C, 46.98; H, 3.21; N, 3.25%.

IR (KBr; ν/cm^{-1}): 3059(w), 1685(vs), 1618(w), 1590(w), 1481 (w), 1436(m), 1364(w), 1278(w), 1241(m), 1186(w), 1171(w), 1156(m), 1141(w), 1092(w), 1016(w), 998(w), 888(w), 821(m), 800(w), 751(m), 707(sh), 692(m), 673(w), 528(s), 507(w), 498 (w), 456(w), 443(w), 436(w).

^{1}H NMR (400 MHz, DMSO-d_6, ppm): δ = 9.50 (d, 1H, J = 8.7 Hz), 8.38 (d, 1H, J = 6.2 Hz), 8.27 (d, 1H, J = 8.3 Hz), 8.02 (t, 1H, J = 7.9 Hz), 7.91 (t, 2H, J = 7.1 Hz), 7.70–7.60 (m, 6H), 7.55 (t, 2H, J = 9.2 Hz), 7.50 (s, 9H), 7.29 (d, 2H, J = 8.0 Hz), 2.30 (s, 3H).

^{13}C NMR (125 MHz, DMSO-d_6): δ = 163.1, 142.4, 141.2, 140.4, 139.3, 138.5, 138.2, 136.9, 134.7, 134.6, 134.0, 133.6, 132.6, 132.5, 131.9, 131.7, 131.6, 131.4, 130.9, 130.7, 129.4, 129.3, 129.2, 128.8, 128.7, 127.8, 126.4, 126.3, 125.6, 124.2, 123.3, 121.9, 119.4, 119.3, 22.4 ppm.

^{31}P NMR (DMSO-d_6): δ = 25.79 ppm.

UV–Vis (MeCN; λ_{max} [nm] (ε; [dm^3 mol^{-1} cm^{-1}])): 761 (89); 587 (225); 464 (1960); 327 (5489); 233 (29378); 190 (59931).

4.5. Crystal structure determination and refinement

The X-ray intensity data of **1**–**8** were collected on a Gemini A Ultra diffractometer equipped with Atlas CCD detector and graphite monochromated Mo Kα radiation (λ = 0.71073 Å) at room temperature. Details concerning crystal data and refinement are given in Tables S1 and S2. Lorentz, polarization and empirical absorption correction using spherical harmonics implemented in SCALE3 ABSPACK scaling algorithm were applied [15]. The structures were solved by the Patterson method and subsequently completed by the difference Fourier recycling. All the non-hydrogen atoms were refined anisotropically using full-matrix, least-squares technique. The hydrogen atoms were treated as "riding" on their parent carbon atoms and assigned isotropic temperature factors equal 1.2 (non-methyl) and 1.5 (methyl) times the value of equivalent temperature factor of the parent atom. The methyl groups were allowed to rotate about their local threefold axis. SHELXS97 and SHELXL97 programs were used for all the calculations [16]. Atomic scattering factors were those incorporated in the computer programs.

4.6. Computational details

The gas phase geometries of **1**, **3**, **5** and **7** were optimized without any symmetry restrictions in singlet ground-states with the DFT method using the hybrid PBE1PBE functional of GAUSSIAN-03 program package [17]. The calculations were performed using ECP LANL2DZ basis set with an additional d and f function with the exponent α = 0.3811 and α = 2.033 for rhenium and the standard 6-31G basis set for other atoms. For chlorine, oxygen, nitrogen and phosphorous atoms, diffuse and polarization functions were added [18]. The optimized geometries of $trans$-(Cl,Cl)-[Re(p-NC$_6$H$_4$CH$_3$)Cl$_2$(4-MeO-quin-2-COO)(PPh$_3$)], cis-(Cl,Cl)-[Re(p-NC$_6$H$_4$CH$_3$)Cl$_2$(4-MeO-quin-2-COO)(PPh$_3$)], $trans$-(Cl,Cl)-[Re(p-NC$_6$H$_4$CH$_3$)Cl$_2$(isoquin-1-COO)(PPh$_3$)] and cis-(Cl,Cl)-[Re(p-NC$_6$H$_4$CH$_3$)Cl$_2$(isoquin-1-COO)(PPh$_3$)] were verified by performing frequency calculation. The absence of imaginary frequency in the calculated vibrational frequencies ensures that the optimized geometries correspond to true energy minima. For the geometry optimizations the initial X-ray structures were used, and all the subsequent calculations were performed based on optimized geometries.

Natural bond orbital (NBO) calculations were performed with the NBO code included in Gaussian03 [19].

4.7. Catalytic oxidations

The reactions of alcohols and hydrocarbons were usually carried out in air in thermostated Pyrex cylindrical vessels with vigorous stirring and using MeCN as solvent. Typically, catalyst and the co-catalyst (acid) were introduced into the reaction mixture in the form of stock solutions in acetonitrile. The substrate (alcohol or hydrocarbon) was then added and the reaction started when TBHP was introduced in one portion. (**CAUTION**. The combination of air or molecular oxygen and peroxides with organic compounds at elevated temperatures may be explosive!). The reactions with 1-phenylethanol were analyzed by ^{1}H NMR method (solutions in acetone-d_6; “Bruker AMX-400” instrument, 400 MHz). Areas of methyl group signals were measured to quantify oxygenates formed in oxidations of 1-phenylethanol. Previously in our works the samples obtained in the alkane oxidation were typically analyzed twice (before and after their treatment with PPh_3) by GC (LKhM-80-6 instrument, columns 2 m with 5% Carbowax 1500 on 0.25–0.315 mm Inerton AW-HMDS; carrier gas argon). This method (an excess of solid triphenylphosphine is added to the samples 10–15 min before the GC analysis) was proposed by one of us earlier [20]. In order to precisely determine concentrations of isomeric alkanols the samples of reaction solutions after addition of nitromethane were analyzed only after reduction with PPh_3. Attribution of peaks was made by comparison with chromatograms of authentic samples.

Acknowledgements

The research was supported by the National Research and Development Center (NCBiR) under Grant ORGANOMET No: PBS2/A5/40/2014, the Russian Foundation for Basic Research (grant 16-03-00254) and the “Science without Borders Program, Brazil–Russia”, CAPES (grant A017-2013). The GAUSSIAN-09 calculations were carried out in the Wrocław Centre for Networking and Supercomputing, WCSS, Wrocław, Poland, http://www.wcss.wroc.pl.

Appendix A. Supplementary material

CCDC 1453422, 1453423, 1453417, 1453420, 1453421, 1453424, 1453418 and 1453419 contains the supplementary crystallographic data for complexes **1**–**8**. These data can be obtained free of charge from The Cambridge Crystallographic Data Centre via www.ccdc.cam.ac.uk/data_request/cif. Supplementary data associated with this article can be found, in the online version, at http://dx.doi.org/10.1016/j.ica.2016.04.030.

References

[1] (a) S.K.-Y. Leung, W.-M. Tsui, J.-S. Huang, C.-M. Che, J.-L. Liang, N. Zhu, J. Am. Chem. Soc. 127 (2005) 16629;
(b) M. Palucki, N.S. Finney, P.J. Pospisil, M.L. Güller, T. Ishida, E.N. Jacobsen, J. Am. Chem. Soc. 120 (1998) 948;
(c) S.-M. Au, J.-S. Huang, W.-Y. Yu, W.-H. Fung, C.-M. Che, J. Am. Chem. Soc. 121 (1999) 9120;
(d) R.E. Cowley, N.A. Eckert, S. Vaddadi, T.M. Figg, T.R. Cundari, P.L. Holland, J. Am. Chem. Soc. 133 (2011) 9796;
(e) C. Besson, J.-H. Mirebeau, S. Renaudineau, S. Roland, S. Blanchard, H. Vezin, C. Courillon, A. Proust, Inorg. Chem. 50 (2011) 2501;
(f) P. Leeladee, G.N.L. Jameson, M.A. Siegler, D. Kumar, S.P. de Visser, D.P. Goldberg, Inorg. Chem. 52 (2013) 4668.
[2] (a) A.K.M. Long, R.P. Yu, G.H. Timmer, J.F. Berry, J. Am. Chem. Soc. 132 (2010) 12228;
(b) W.-L. Man, W.W.Y. Lam, S.-M. Yiu, T.-C. Lau, S.-M. Peng, J. Am. Chem. Soc. 126 (2004) 15336;
(c) S. Abbina, S. Bian, C. Oian, G. Du, ACS Catal. 3 (2013) 678;
(d) W.-L. Man, W.W.Y. Lam, T.-C. Lau, Acc. Chem. Res. 47 (2014) 427;
(e) J. Wang, L. Huang, X. Yang, H. Wei, Organometallics 34 (2015) 212.
[3] (a) W.A. Herrmann, R.W. Fischer, J.D.G. Correia, J. Mol. Catal. 94 (1994) 213;
(b) E.A. Ison, E.R. Trivedi, R.A. Corbin, M.M. Abu-Omar, J. Am. Chem. Soc. 127 (2005) 15374;
(c) G. Du, P.E. Fanwick, M.M. Abu-Omar, J. Am. Chem. Soc. 129 (2007) 5180;
(d) K.R. Jain, W.A. Herrmann, F.E. Kühn, Coord. Chem. Rev. 252 (2008) 556;
(e) M. Crucianelli, R. Saladino, F. De Angelis, ChemSusChem 3 (2010) 524;
(f) M.-J. Cheng, Dalton Trans. 41 (2012) 3758;
(g) E.C.B.A. Alegria, L.M.D.R.S. Martins, M.V. Kirillova, A.J.L. Pombeiro, Appl. Cat. A: General 443–444 (2012) 27–32;
(h) L.M.D.R.S. Martins, E.C.B.A. Alegria, P. Smoleński, M.L. Kuznetsov, Inorg. Chem. 52 (2013) 4534.
[4] (a) U. Schuchardt, D. Mandelli, G.B. Shul’pin, Tetrahedron Lett. 37 (1996) 6487;
(b) G. Bianchini, M. Crucianelli, F. De Angelis, V. Neri, R. Saladino, Tetrahedron Lett. 45 (2004) 2351;
(c) G. Bianchini, M. Crucianelli, F. De Angelis, V. Neri, R. Saladino, Tetrahedron Lett. 46 (2005) 2427;
(d) A.M. Kirillov, M. Haukka, M.F.C. Guedes da Silva, A.J.L. Pombeiro, Eur. J. Inorg. Chem. (2005) 2071;
(e) E.C.B. Alegria, M.V. Kirillova, L.M.D.R.S. Martins, A.J.L. Pombeiro, Appl. Catal. A: Gen. 317 (2007) 43;
(f) M.L. Kuznetsov, A.J.L. Pombeiro, Inorg. Chem. 48 (2009) 307;
(g) E.A. Karlsson, T. Privalov, Chem. Eur. J. 15 (2009) 1862;
(h) M. Carril, P. Altmann, M. Drees, W. Bonrath, T. Netscher, J. Schütz, F.E. Kühn, J. Catal. 283 (2011) 55;
(i) M. Carril, P. Altmann, W. Bonrath, T. Netscher, J. Schütz, F.E. Kühn, Sci. Technol. 2 (2012) 722;
(j) T. Hwang, B.R. Goldsmith, B. Peters, S.L. Scott, Inorg. Chem. 52 (2013) 13904;
(k) L.M.D.R.S. Martins, A.J.L. Pombeiro, Coord. Chem. Rev. 265 (2014) 74.
[5] (a) H.H. Nguyen, C.T. Pham, U. Abram, Polyhedron 99 (2015) 216;
(b) X. Schoultz, T.I.A. Gerber, E. Hosten, R. Betz, L. Rhyman, P. Ramasami, Polyhedron 96 (2015) 6;
(c) S. Banerjee, S. Bhattacharyya, B. Kumar Dirghangi, M. Menon, A. Chakravorty, Inorg. Chem. 39 (2000) 6;
(d) I. Booysen, T.I.A. Gerber, E. Hosten, P. Mayer, Z.R. Tshentu, J. Coord. Chem. 60 (2007) 1771;
(e) T.I.A. Gerber, D.G. Luzipo, P. Mayer, J. Coord. Chem. 59 (2006) 1515;
(f) R.A. Eikey, M.M. Abu-Omar, Coord. Chem. Rev. 243 (2003) 83.
[6] U. Abram, R. Alberto, J. Braz. Chem. Soc. 17 (2006) 1486.
[7] (a) B. Machura, M. Wolff, A. Świtlicka, I. Gryca, Polyhedron 29 (2010) 2381;
(b) B. Machura, M. Wolff, I. Gryca, Polyhedron 30 (2011) 142;
(c) B. Machura, M. Wolff, I. Gryca, Inorg. Chim. Acta 370 (2011) 7;
(d) B. Machura, I. Gryca, M. Wolff, Polyhedron 31 (2012) 128;
(e) B. Machura, I. Gryca, Polyhedron 53 (2013) 83;
(f) B. Machura, I. Gryca, J.G. Małecki, F. Alonso, Y. Moglie, Dalton Trans. 43 (2014) 2596;
(g) I. Gryca, B. Machura, J.G. Małecki, L.S. Shul’pina, A.J.L. Pombeiro, G.B. Shul’pin, Dalton Trans. 43 (2014) 5759;
(h) I. Gryca, B. Machura, J.G. Małecki, J. Kusz, L.S. Shul’pina, N.S. Ikonnikov, G.B. Shul’pin, Dalton Trans. 45 (2016) 334.
[8] (a) G.B. Deacon, R.J. Phillips, Coord. Chem. Rev. 33 (1980) 227;
(b) K. Nakamoto, Infrared and Raman Spectra of Inorganic and Coordination Compounds, fourth ed., Wiley-Interscience, New York, 1986.
[9] (a) R. Rossi, A. Marchi, A. Duatti, L. Magon, U. Casellato, R. Graziani, G. Polizzotti, Inorg. Chim. Acta 90 (1984) 121;
(b) V.M. Bereau, S.I. Khan, M.M. Abu-Omar, Inorg. Chem. 40 (2001) 6767.
[10] (a) M.T. Ahmet, B. Coutinho, J.R. Dilworth, J.R. Miller, S.J. Parrott, Y. Zheng, Polyhedron 15 (1996) 2041;
(b) P. Mayer, E. Hosten, K.C. Potgieter, T.I.A. Gerber, J. Chem. Crystallogr. 40 (2010) 1146.
[11] S.R. Flechter, A.C. Skapski, J. Chem. Soc., Dalton Trans. (1972) 1073.
[12] (a) L. Wei, J. Zubieta, J.W. Babich, Inorg. Chem. 43 (2004) 6445;
(b) G. Bandoli, T.I.A. Gerber, J. Perils, J.G.H. du Preez, Inorg. Chim. Acta 278 (1998) 96;
(c) G. Bandoli, A. Dolmella, T.I.A. Gerber, J. Perils, J.G.H. du Preez, Bull. Chem. Soc. Ethiop. 16 (2002) 149;
(d) B. Machura, R. Kruszynski, M. Jaworska, Polyhedron 24 (2005) 1454.
[13] (a) M.V. Kirillova, A.M. Kirillov, D. Mandelli, W.A. Carvalho, A.J.L. Pombeiro, G. B. Shul’pin, J. Catal. 272 (2010) 9;
(b) A.M. Kirillov, M.V. Kirillova, L.S. Shul’pina, P.J. Figiel, K.R. Gruenwald, M.F.C. G. da Silva, M. Haukka, A.J.L. Pombeiro, G.B. Shul’pin, J. Mol. Catal. A: Chem. 350 (2011) 26;
(c) M.M. Vinogradov, Y.N. Kozlov, A.N. Bilyachenko, D.S. Nesterov, L.S. Shul’pina, Y.V. Zubavichus, A.J.L. Pombeiro, M.M. Levitsky, A.I. Yalymov, G.B. Shul’pin, New J. Chem. 39 (2015) 187;
(d) V.B. Romakh, B. Therrien, G. Süss-Fink, G.B. Shul’pin, Inorg. Chem. 46 (2007) 1315.
[14] J. Chatt, J.D. Garforth, N.P. Johnson, G.A. Rowe, J. Chem. Soc. (1964) 1012.

Please cite this article in press as: I. Gryca et al., Inorg. Chim. Acta (2016), http://dx.doi.org/10.1016/j.ica.2016.04.030

[15] CRYSALIS RED, Version 1.171.33.46, Oxford Diffraction Ltd., 2003.
[16] G.M. Sheldrick, Acta Crystallogr., Sect. A A64 (2008) 112.
[17] M.J. Frisch, G.W. Trucks, H.B. Schlegel, G.E. Scuseria, M.A. Robb, J.R. Cheeseman, G. Scalmani, V. Barone, B. Mennucci, G.A. Petersson, H. Nakatsuji, M. Caricato, X. Li, H.P. Hratchian, A.F. Izmaylov, J. Bloino, G. Zheng, J.L. Sonnenberg, M. Hada, M. Ehara, K. Toyota, R. Fukuda, J. Hasegawa, M. Ishida, T. Nakajima, Y. Honda, O. Kitao, H. Nakai, T. Vreven, J.A. Montgomery Jr., J.E. Peralta, F. Ogliaro, M. Bearpark, J.J. Heyd, E. Brothers, K.N. Kudin, V.N. Staroverov, R. Kobayashi, J. Normand, K. Raghavachari, A. Rendell, J.C. Burant, S.S. Iyengar, J. Tomasi, M. Cossi, N. Rega, J.M. Millam, M. Klene, J.E. Knox, J.B. Cross, V. Bakken, C. Adamo, J. Jaramillo, R. Gomperts, R.E. Stratmann, O. Yazyev, A.J. Austin, R. Cammi, C. Pomelli, J.W. Ochterski, R.L. Martin, K. Morokuma, V.G. Zakrzewski, G.A. Voth, P. Salvador, J.J. Dannenberg, S. Dapprich, A.D. Daniels, O. Farkas, J.B. Foresman, J.V. Ortiz, J. Cioslowski, D.J. Fox, Gaussian 09, Revision A.1, Gaussian Inc., Wallingford CT, 2009.
[18] (a) P.J. Hay, W.R. Wadt, J. Chem. Phys. 82 (1985) 299;
(b) K. Eichkorn, F. Weigend, O. Treutler, R. Ahlrichs, Theor. Chem. Acc. 97 (1997) 119;
(c) P.M.W. Gill, B.G. Johnson, J.A. Pople, M.J. Frisch, Chem. Phys. Lett. 197 (1992) 499.
[19] (a) NBO Version 3.1, E. D. Glendening, A. E. Reed, J. E. Carpenter, F. Weinhold.;
(b) E. Reed, L.A. Curtiss, F. Weinhold, Chem. Rev. 88 (1988) 899.
[20] (a) G.B. Shul'pin, A.N. Druzhinina, React. Kinet. Catal. Lett. 47 (1992) 207;
(b) G.B. Shul'pin, G.V. Nizova, React. Kinet. Catal. Lett. 48 (1992) 333;
(c) G.B. Shul'pin, J. Mol. Catal. A: Chem. 189 (2002) 39;
(d) G.B. Shul'pin, C. R. Chim. 6 (2003) 163;
(e) G.B. Shul'pin, Mini-Rev. Org. Chem. 6 (2009) 95;
(f) G.B. Shul'pin, Y.N. Kozlov, L.S. Shul'pina, A.R. Kudinov, D. Mandelli, Inorg. Chem. 48 (2009) 10480;
(g) G.B. Shul'pin, Org. Biomol. Chem. 8 (2010) 4217;
(h) G.B. Shul'pin, Y.N. Kozlov, L.S. Shul'pina, P.V. Petrovskiy, Appl. Organometal. Chem. 24 (2010) 464;
(i) G.B. Shul'pin, Dalton Trans. 42 (2013) 12794;
(j) G.B. Shul'pin, Catalysts 6 (2016) paper No. 50.

Please cite this article in press as: I. Gryca et al., Inorg. Chim. Acta (2016), http://dx.doi.org/10.1016/j.ica.2016.04.030